International Journal of Heat and Technology
Vol. 42, No. 4, August, 2024, pp. 1231-1239
Journal homepage: http://iieta.org/journals/ijht

Thermal-Hydraulic Performance of Additively Manufactured Plate Heat Exchangers with Single and Double Sine Wave Corrugations: A CFD Study

Ahmed M. Alshwairekh

Department of Mechanical Engineering, College of Engineering, Qassim University, Qassim 52571, Saudi Arabia

Corresponding Author Email: shoierkh@qu.edu.sa

https://doi.org/10.18280/ijht.420413

Received: 6 June 2024
Revised: 21 July 2024
Accepted: 2 August 2024
Available online: 31 August 2024

Keywords:
CFD, heat exchangers, low-temperature heat exchangers, 3D printing, Nusselt number, friction factor

ABSTRACT

Computational fluid dynamics (CFD) simulations were employed to model a novel double sine wave corrugated heat exchanger surface. The turbulent flow within the heat exchanger channels was simulated using the *k-ω SST* model for the corrugated cases. In contrast, a laminar model was applied to the flat plate heat exchanger without corrugations. The simulation results demonstrate that 3D-printed polymer heat exchangers are effective for heat transfer, with the double-sine wave corrugated surface outperforming the single-sine wave corrugated surface. Specifically, the double sine wave configuration achieved a 20% higher Nusselt number and a 15% lower friction factor than the single sine wave, indicating superior thermal-hydraulic performance. Optimal performance was observed with low amplitude and frequency of the sine waves, suggesting that small protrusions and wider-spaced corrugations enhance heat transfer without significantly increasing pressure drop. These findings have significant implications for the design of efficient and cost-effective heat exchangers, particularly in applications where both thermal performance and energy efficiency are critical. Further experiments with full-scale heat exchangers are necessary to validate these results and explore practical applications.

1. INTRODUCTION

Heat exchangers (HXs) are designed to transfer thermal energy between two or more fluids without mixing them [1]. Several factors influence the performance of heat exchangers, one of which is the level of turbulence in the fluid streams. Increased turbulence enhances momentum mixing, thereby improving thermal energy transfer between the fluids within the heat exchanger.

The heat exchanger design has relied heavily on the use of metals since the thermal conductivity of metal is high. Also, metals have several other advantages, such as mechanical strength and high tolerance to heat. Utilizing the high thermal conductivity in metals in the design of HXs is not enough, and turbulators are usually added to enhance the momentum mixing of the fluids to increase the heat transfer rate. The addition of turbulators or corrugations is accompanied by an increase in the pressure drop inside the HX. This is considered an adverse effect on the design of HXs. However, the shape and location of such turbulators play an essential role in the ratio of heat transfer enhancements to the increase in the pressure drop inside the HX. It is desired that the heat transfer rate inside HXs be increased with little increase in the pressure drop.

Several researchers have investigated the use of turbulators in the design of HXs. Nakhchi et al. [2] experimentally investigated using a double-perforated inclined elliptic turbulator to enhance the heat transfer in a double-pipe HX. The perforation helps reduce pressure loss, helps mix the fluid, and disrupts the thermal boundary layer. The angle of inclination and the diameter of the perforations varied in their study with different flow rates in the turbulent regime. They found that, at best, the heat transfer was enhanced by 39.4%. Moria [3] numerically investigated using a spring wire with different cross-sections as the turbulator element inside a spiral tube HX. The results indicated that the triangular cross-section had the best influence on increasing the Nusselt number and thermal-hydraulic performance. Samruaisin et al. [4] experimentally investigated using V-shaped delta-wing baffles inside a round tube to enhance the heat transfer. The experiment consisted of different numbers of wings and different pitch levels. Their results indicated that using eight wings resulted in a high level of mixing and a 138.9% increase in the Nusselt number. Several researchers [5-7] had come to the same conclusion that adding turbulators will increase the heat transfer rate in HXs. However, care should be taken to avoid excessive pressure drop inside HXs.

Recently, additive manufacturing (AM) has gained interest in the engineering community [8]. AM has several benefits over traditional manufacturing techniques [9]. AM is sometimes referred to as rapid prototyping because of the quick production of physical parts from computer-aided design software [10]. Designs can be physically manufactured in-house using as little as one manufacturing device and without post-processing. Most polymer AM technology is widely used among professional engineers and amateurs. However, metal AM technologies are limited to professional engineers and companies as these technologies are still

expensive and difficult to operate [11].

Several researchers are using AM technology to design and enhance HXs. Alshwairekh [12] numerically studied the thermal-hydraulic performance of AM flat plate HXs with corrugations. The geometry consisted of several turbulators in the shape of a hemisphere located along the HX. The results indicate thermal-hydraulic performance improves when the turbulators are further spaced apart with small protrusions. Lorenzon et al. [13] experimentally investigated the use of pin-fins in annular channels for cooling. They used different dimensions of the pin-fin to test the thermal-hydraulic performance of the pin-fin cooling. Their results indicated that the largest height-to-pin diameter ratio is better for thermal performance.

This research article aims to study the effect of sine and double sine wave corrugation inside HXs. The sine wave-like corrugations work as turbulators to the flow inside the HX channels. The addition of turbulators will increase the pressure drop inside the HX. However, the overall thermal-hydraulic performance of the HX will be assessed and presented. A series of two-dimensional CFD simulations were carried out to study the effect of double and single sine corrugations and flow rate on the thermal performance of the HXs.

This paper is structured as follows:

- **Mathematical Model**: I detail the theoretical principles and mathematical formulations used to describe the heat transfer and fluid flow in the heat exchanger.
- **Numerical Model**: I present the numerical methods, geometry, and simulations employed to model the heat exchanger configurations and predict their performance.
- **Results and Discussion**: The simulation results are analyzed, the performance of different corrugated surfaces is compared, and the implications of the findings are discussed.
- **Conclusion**: I summarize the key findings, practical implications, and potential directions for future research.

2. MATHEMATICAL MODEL

Navier-Stokes, energy, and the conservation of mass equations are used to model the fluid flow and heat transfer inside the additively manufactured HX.

The conservation of mass equation as:

$$\frac{\partial u_i}{\partial x_i} = 0 \tag{1}$$

The conservation of momentum equation as:

$$u_j \frac{\partial u_i}{\partial x_j} = -\frac{1}{\rho}\frac{\partial p}{\partial x_i} + \frac{1}{\rho}\frac{\partial}{\partial x_j}\left(\mu \frac{\partial u_i}{\partial x_j}\right) \tag{2}$$

The energy equation as:

$$u_j \frac{\partial T}{\partial x_j} = \frac{k}{\rho c_p}\frac{\partial}{\partial x_j}\left(\frac{\partial T}{\partial x_j}\right) \tag{3}$$

where, ρ is the fluid density, p is the fluid pressure, μ is the fluid viscosity, T is the absolute temperature of the fluid, k is the thermal conductivity of the fluid, and c_p is the specific heat of the fluid inside the HX. u_i is the velocity vector, and i and j are tensorial indices that change depending on the dimensions of the geometry used. In the current study, only two dimensions are considered.

One of the distinctive features of additively manufactured HXs is the inherent roughness of HX walls due to the layer stacking caused by the AM technique. As the fluid flows inside the HX, turbulent flow occurs due to the roughness of the walls. Laminar flow might be obtained inside the HX if the flow rate is low enough. However, as the flow rate increases, the flow regime inside the HX becomes turbulent.

Directly solving the Navier-Stokes equations without any assumptions in turbulence simulations is computationally expensive. This approach is commonly called direct numerical simulation (DNS). To make the simulations easier, models are used to model turbulence in fluid flow. The *k-ω* shear stress transport (*k-ω SST*) turbulence model will be used to simulate the high-flow rate cases [14, 15]. The *k-ω* shear stress transport model equations are given as:

$$u_j \frac{\partial u_i}{\partial x_j} = -\frac{1}{\rho}\frac{\partial p}{\partial x_i} + \frac{1}{\rho}\frac{\partial}{\partial x_j}\left((\mu + \mu_t)\frac{\partial u_i}{\partial x_j}\right) \tag{4}$$

$$u_j \frac{\partial T}{\partial x_j} = \frac{\partial}{\partial x_j}\left(\left(\frac{k}{\rho c_p} + \frac{\mu_t}{\rho\, Pr_t}\right)\frac{\partial T}{\partial x_j}\right) \tag{5}$$

where, Pr_t is the turbulent Prandtl number, and $\mu_t = \rho \frac{a_1 k}{max(a_1\omega, \mathrm{S}\, F_2)}$ is the eddy viscosity and S is the vorticity magnitude.

The turbulent kinetic energy equation k is given as:

$$u_i \frac{\partial(\rho k)}{\partial x_i} = \tau_{ij}\frac{\partial u_i}{\partial x_j} - \beta^* \rho\omega k + \frac{\partial}{\partial x_j}\left((\mu + \sigma_k \mu_t)\frac{\partial k}{\partial x_j}\right) \tag{6}$$

The specific dissipation rate ω is given as:

$$u_i \frac{\partial(\rho\omega)}{\partial x_i} = \frac{\gamma}{\upsilon_t}\tau_{ij}\frac{\partial u_i}{\partial x_j} - \beta\rho\omega^2 + \frac{\partial}{\partial x_j}\left[(\mu + \sigma_\omega \mu_t)\frac{\partial \omega}{\partial x_j}\right] + 2\rho(1 - F_1)\sigma_{\omega 2}\frac{1}{\omega}\frac{\partial k}{\partial x_j}\frac{\partial \omega}{\partial x_j} \tag{7}$$

where, γ, a_1, β, β^*, σ_k, σ_ω, and $\sigma_{\omega 2}$ are closure coefficient and F_1, F_2 are blending functions. More details about the model can be found in the paper by Menter [14].

Heat exchangers typically run for long periods; thus, they can be modeled as steady-state devices. The first law of thermodynamics can be applied to the heat exchanger, and the following equation can be used to estimate the amount of heat transfer between the hot and cold channels of the HX:

$$\dot{Q} = \dot{m}_c\, c_{pc}\left(T_{c,\,out} - T_{c,\,in}\right) \text{ or } \dot{Q} = \dot{m}_h\, c_{ph}\left(T_{h,\,in} - T_{h,\,out}\right) \tag{8}$$

where, the mass flow rate in the cold or hot channels is $\dot{m}$ with the appropriate subscript. The specific heat is generally variable with temperature, but it can be assumed as a single value for the average temperature range the HX works at, and it is given as c_p. The temperatures of the inlet and outlets to the HX channels are given as T. The temperature variation along the inlet and outlet of the HX is variable. Eq. (8) assumes an average value over the inlet and outlet of the HX. Another

approach to calculate the heat transfer rate is to use the concept of overall heat transfer coefficient as:

$$\dot{Q} = U\,A\,\Delta T_{lm} \tag{9}$$

where, A is the heat transfer area and U is the overall heat transfer coefficient, which is defined as $U = \frac{1}{h_i A_i} + R_{wall} + \frac{1}{h_o A_o}$ and ΔT_{lm} is the log mean temperature difference, and it is defined as:

$$\Delta T_{lm} = \frac{\Delta T_1 - \Delta T_2}{\ln(\Delta T_1/\Delta T_2)} \tag{10}$$

The average Nusselt number inside the HX can be calculated using the following equation:

$$Nu = \frac{hD}{k} \tag{11}$$

where, h is the convective heat transfer coefficient, k is the thermal conductivity of the water and D is the hydraulic diameter of the HX. The friction factor within the HX channel was estimated by the following equation:

$$f = \frac{2\,D\,\Delta P}{L\,\rho\,V^2} \tag{12}$$

The thermal-hydraulic performance is estimated using the following equation:

$$THP = \frac{Nu/Nu_e}{(f/f_e)^{1/3}} \tag{13}$$

where, the subscript e denotes the case with no corrugations or empty.

2.1 Numerical model and geometry

The geometry used consists of a two-dimensional section of a flat plate HX. Since the flow inside the HX is dominated by a streamwise flow, the two-dimensional representation of the HX allows a simplification of the simulations. To reduce computational power, the HX is represented using only two channels. One channel has the hot liquid stream, while the other has the cold liquid stream. The flow of the liquids in the HX is counter-current flow. The wall separating the two channels allows for the energy exchange between the two fluid streams in the form of conduction heat transfer. A polymer-based material is used in the simulated cases. Therefore, the thermal conductivity of the HX wall is considered low. However, there are several applications where polymer heat exchangers are needed, as demonstrated by Li et al. [16] and Ahmad et al. [17]. The heat exchange between the hot and cold fluid streams can be modeled using a thermal resistance concept connected in series. The convection resistance in the hot and cold fluid streams is given as:

$$R_{conv} = \frac{1}{hA_s} \tag{14}$$

where, h is the convective heat transfer coefficient in the hot or cold liquid stream and A_s is the HX surface area. Also, the thermal resistance due to conduction within the HX wall is given as:

$$R_{cond} = \frac{t}{k_p A_s} \tag{15}$$

where, t is the thickness of the HX wall, k_p is the thermal conductivity of the polymer-based HX, and A_s is the surface area of the HX. The conduction thermal resistance in metal HXs is usually neglected. However, if the HX is constructed using polymer-based material, the conduction resistance might be high and should be considered. Having a thin-walled HX will reduce the conduction resistance to a negligible value.

The thermal resistance to heat transfer should be reduced to enhance the heat transfer rate in the HX. One way of reducing the thermal resistance is to increase the surface area of the HX since the surface area is inversely proportional to the thermal resistance. The other way is to increase the convective heat transfer coefficient either in the hot or the cold channels since the heat transfer convective coefficient is also inversely proportional to the thermal resistance to heat transfer. The flow velocity can be increased to increase the heat transfer convective coefficient in the HX. Still, there might be limitations to the increase in the flow velocity, which depends on the system where the HX operates. The best way of increasing the convective heat transfer coefficient in the HX is to add corrugations that disrupt the growth of the thermal boundary layer in the streamwise direction.

Great effort has been made to introduce corrugations in the design of HXs. However, there is room for improvement in the heat transfer rate in HXs. Recently, Additive manufacturing started to emerge as a manufacturing technique. One of the advantages of additive manufacturing is the ability to manufacture complicated shapes that were not possible with conventional means of manufacturing. This allows HX designers to use complex geometries to enhance the convective heat transfer coefficient, which was overlooked before due to geometric complexities.

One method of wall corrugation is the use of sine wave-like corrugations. This type of corrugation has been studied extensively before [18-20]. However, to the best of my knowledge, a series of sine waves with different amplitudes and frequencies has never been used as wall corrugations before. To produce a HX wall with several sine waves, the profile of the corrugated wall is defined as:

$$y = \sum_{n=1}^{\infty} A_n \sin(\omega_n x) \tag{16}$$

where, A_n is the amplitude and ω is the frequency. Mathematically, an infinite number of sine terms with different amplitudes and frequencies can be used. However, practical limitations might arise, which depend on the difficulty of manufacturing, even with the help of additive manufacturing. Therefore, only two sine terms are considered in this study:

$$y = A_1 \sin(\omega_1 x) + A_2 \sin(\omega_2 x) \tag{17}$$

The values for the amplitudes and frequencies should be chosen carefully to increase the convective heat transfer coefficient while maintaining a relatively low increase in pressure drop due to the introduction of these corrugations.

Figure 1 shows the profile of the two-term sine wave used as a corrugation in the HX wall.

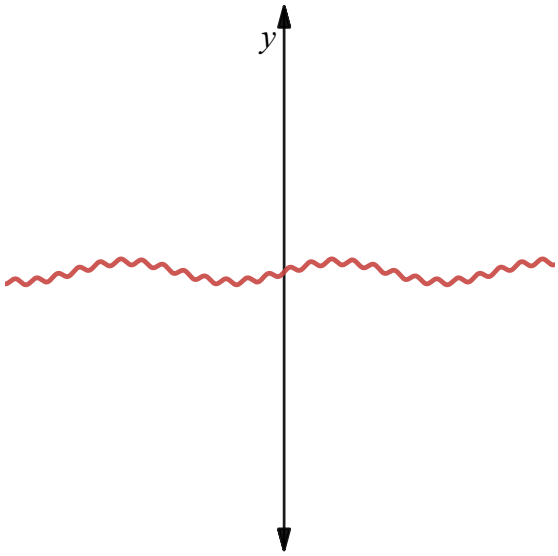

Figure 1. The profile of a two-term sine wave with $A_1 = 1$, $\omega_1 = 0.3$, $A_2 = 0.3$, $\omega_1 = 3$

The profile of the HX wall seems random, except it is well-defined using the two-term sine wave equation. The equation is periodic and can be extended to any length required in the streamwise direction.

The two-dimensional representation of a flat plate HX is shown in Figure 2. Only two channels are considered for the current study. The height of each channel of the HX is set to be 3 mm. The wall separating the two channels is the surface where the heat transfer occurs; therefore, the wall is corrugated in a two-term sine wave pattern. Two amplitudes and two frequencies characterize the corrugations. The values used in the current simulations are summarized in Table 1. The first sine wave has a high amplitude and a low frequency, while the second sine wave has a high frequency and low amplitude, as shown in Table 1. This combination should produce good momentum mixing near the HX wall and disrupt the growth of the thermal boundary layer, maintaining a relatively low increase in pressure drop. SolidWorks was used to produce the corrugated surface using the equation-driven curve command. The geometry is then exported to the Ansys design modeler for further preprocessing.

Table 1. Values used for the amplitude and the frequencies in the two-term sine wave corrugated HX wall

Geometry	A_1 [mm]	ω_1	A_2[mm]	ω_2
Single sine	0.8	0.5	-	-
Double sine 1	0.8	0.5	0.2	2
Double sine 2	0.8	0.25	0.2	1

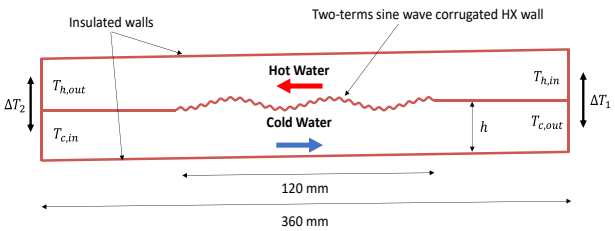

Figure 2. Two-dimensional representation of a flat plate HX

The flow inside the HX is turbulent as the corrugated wall will promote mixing inside the two channels. The peak shape of the corrugation in one channel will form a dip in the adjacent channel and vice versa. Usually, the dips form dead spots where the flow might be stagnant, which is undesirable. This is why the high-frequency sine waves are given low amplitudes to avoid the formation of dead spots in the HX channel. Also, the high amplitude sine wave is formed with low frequency to allow mixing within the dips of the sine wave. Furthermore, the values of Reynold number are varied as: 1500, 2500, and 3500. The Reynold number is calculated as:

$$Re = \frac{\rho V h}{\mu} \tag{18}$$

where, ρ is the water density, V is the average inlet velocity to either channel, h is the height of the channel, and μ is the dynamic viscosity of the water. The density and viscosity are assumed to be constant.

The physical properties of the water are assumed to be constant, and the Reynold number is varied by changing the inlet velocity to the channels. The physical properties of the water and the polymer-based HX are given in Table 2. The polymer-based material is adapted from the company (TCPOLY) named Ice9^{TM} [21].

Table 2. Physical properties of water and the polymer material used in the current simulations

Water	ρ	998.2 kg/m^3
	μ	1003×10^{-6} kg/m · s
	k	0.6 W/m · K
Polymer Material	k_p	6 W/m · K
	ρ_p	1400 kg/m^3
	c_p	1300 J/(kg · K)
	T_{max}	110 ℃

2.2 Boundary conditions and mesh

The boundary conditions for the simulations are an inlet velocity boundary condition to the inlet of both channels. The velocity is varied to maintain the mentioned values of the Reynold number with the constant physical properties and the height of the channel. The inlet temperature of the hot water stream is set to be 350 K while the inlet temperature of the cold-water stream is set to 293 K. The upper wall of the hot water stream and the lower wall of the cold water stream are treated as an insulated wall. The wall that separates the two channels is considered a functional surface with zero thickness in geometry. However, the thickness of the HX wall is given a value of 1 mm inside the simulation's parameters. The heat transfer between the two channels is due to conduction through the corrugated HX surface. Since the flow is treated as turbulent, the inlet turbulent intensity to both channels is set to 5%.

A structured mesh was used to discretize the two-dimensional geometry into smaller cells. After the solution converges, the solution of the governing equations is given in every mesh cell. Since temperature variation and flow are mixing near the HX surface, a refined mesh was used near the corrugated surface. Inflation layers were used near the HX surface, with five layers capturing the formation and disruption of the thermal boundary layer.

Ansys fluent is used to run the simulations of the corrugated

HX. The simulations are treated as steady-state simulations with constant physical properties. The SIMPLE algorithm is used for the pressure-velocity coupling. A second-order upwind scheme is used for the spatial discretization of the governing equations. The simulations were run until residuals reached a value of 1.0×10^{-6} for all governing equations. The current CFD model has already been validated, and a mesh study has been performed. It can be found in my previous publication [12].

3. RESULTS AND DISCUSSIONS

Introducing sine wave corrugations promotes turbulence inside the HX channels, significantly impacting the flow dynamics and heat transfer performance. The following analysis provides a comprehensive examination of the effects of these corrugations through detailed contour plots. Several contours are presented and discussed to better understand the influence of these corrugations on the performance of HXs. It is to be noted that the contours shown in the following figures are scaled down in the x-axis to better fit the entire figure on one page.

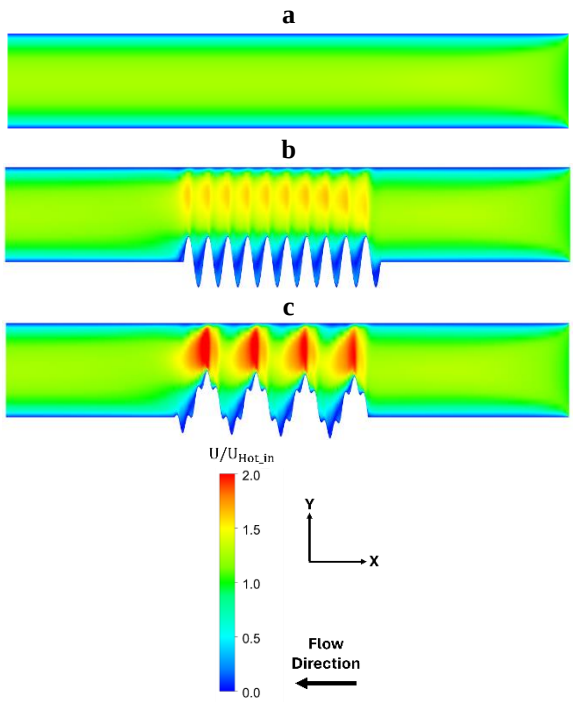

Figure 3. Normalized velocity at Re = 3500 for (a) Flat HX, (b) Single sine wave HX, and (c) Double sine wave HX

Figure 3 shows the contours of the normalized velocity inside the hot channel of the HX. The velocity is normalized using the inlet velocity of the hot channel. The flow of water is from right to left, as shown in the figure by the arrow. Figure 3(a) represents the normalized velocity in an HX with no sine wave corrugations. The walls of the HX are smooth, and no high turbulence is present. As can be seen from the figure, the velocity of water is zero at the top and bottom surfaces of the HX, and the highest value of the normalized velocity is in the middle of the HX channel, as expected. The flow of water is not interrupted since no corrugations are present. Figure 3(b) shows the single sine wave corrugation case. Initially, the flow is not different from the empty case since no corrugations are present. As the flow touches the sine wave corrugations, turbulence happens, and the streamwise velocity changes rapidly near the corrugations. Inside the dips of the sine waves, the velocity is low. However, the average normalized velocity is high over the surface of the HX. High velocity correlates well with an increase in the convective heat transfer coefficient. Figure 3(c) shows the double sine wave corrugation case. The unique feature of this case is the presence of secondary waves from the second sine wave. The secondary waves enhance the momentum mixing inside the HX channel. However, this adds to the pressure drop. Nevertheless, carefully selecting the frequency and amplitude of the two sine parameters can induce high momentum mixing with a relatively low-pressure drop, which resembles the empty case. Like the single sine wave corrugations, the normalized velocity is low in the dips. Still, the average normalized velocity is higher over the HX surface, which indicates a better heat transfer coefficient.

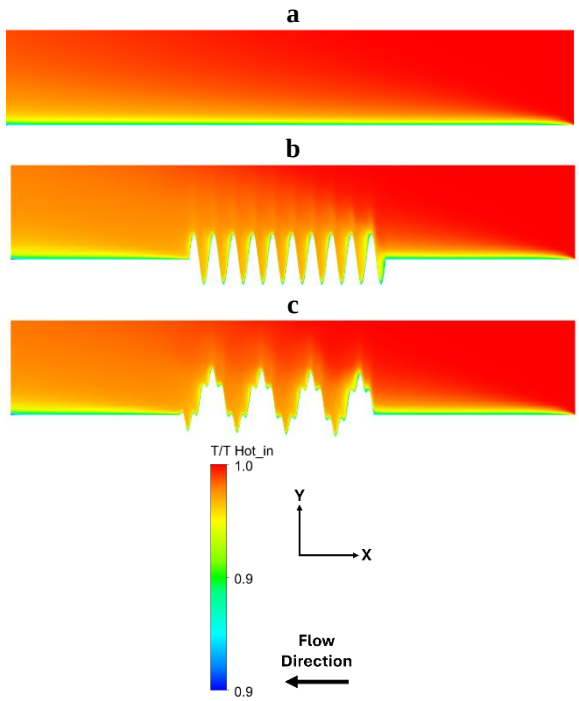

Figure 4. Normalized temperature at Re = 3500 for (a) Flat HX, (b) Single sine wave HX, and (c) Double sine wave HX

Figure 4 shows the normalized temperature contours inside the hot channel of the HX. The contours are normalized using the inlet temperature of the hot channel. The water enters the HX from the right and exits from the left. As the water enters, it exchanges heat with the cold bottom channel. For this reason, the temperature decreases at the bottom of the hot HX channel. A thermal boundary layer develops on the bottom surface as the water flows in the HX channel. The thermal boundary layer presents a resistance to the heat transfer from the hot to the cold channel since the temperature difference decreases. This heat transfer reduction increases as the water flows to the exit of the hot channel. Corrugations are used to break the buildup of the thermal boundary layer. Figure 4(b) shows the single sine wave corrugations. The thermal boundary layer increases with streamwise distance, and as soon as the water touches the corrugations, the thermal boundary layer breaks, and good mixing happens. The mixing allows the hot water at the top of the hot HX channel to contact the bottom surface to increase the heat transfer rate. Once the corrugations are finished, the

thermal boundary layer starts to build up again until the water exits the hot channel of the HX. Figure 4(c) shows the double sine wave corrugations. Secondary corrugation allows for better mixing of the water near the HX surface. Hot spots can be seen along the corrugations, while cold spots are visible by the green color inside the dips. Therefore, lowering the dips formed by the corrugations might be a better option to increase the heat transfer rate for the HX. When comparing the contours of Figure 3 and Figure 4, it is evident that low-velocity spots correspond to colder temperatures, which is undesirable in the hot channel of the HX. However, having this result is reassuring as it acts as one form of results validation.

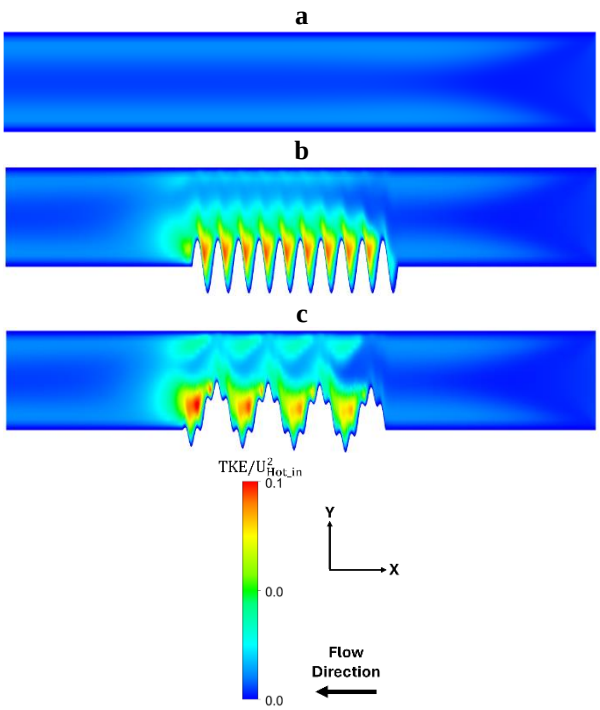

Figure 5. Normalized turbulent kinetic energy at Re = 3500 for (a) Flat HX, (b) Single sine wave HX, and (c) Double sine wave HX

Figure 5 shows the contours of the normalized kinetic energy inside the hot channels of the HX. The contours are normalized with the square of the inlet velocity to the hot channel. The turbulent kinetic energy measures how big the turbulent is inside the channel. Since there are no mixing promotors in the empty channel, the turbulent kinetic energy is not high, and the flow is not turbulent. Figure 5(b) shows the single sine wave mixing promoters and how their presence gives rise to turbulence near the HX surface. Similarly, Fig. 5(c) shows the double sine corrugations mixing promoters and how they create turbulence near the HX surface. The presence of the eddies helps mitigate the formation of the thermal boundary layer and enhances the heat transfer within the HX.

The increase in TKE due to the presence of sine wave corrugations can be credited to the generation of flow instabilities and eddies. These turbulent structures facilitate enhanced water mixing, leading to more uniform temperature distribution and improved heat transfer rates. The double sine wave configuration, with its secondary waves, creates additional points of flow separation and reattachment, further increasing turbulence and enhancing heat transfer.

The results are consistent with our previous study on turbulent flow in membrane corrugated channels, for example, Alshwairekh et al. [22] showed that channel corrugations can improve the mass transfer within membrane systems. However, my current study focuses on the special nature of the double sine wave corrugations, which gives better control over the level of mixing based on the different variables involved. The additional turbulence generated by the secondary waves in the double sine wave resulted in higher TKE levels and better heat transfer performance than single sine wave corrugations.

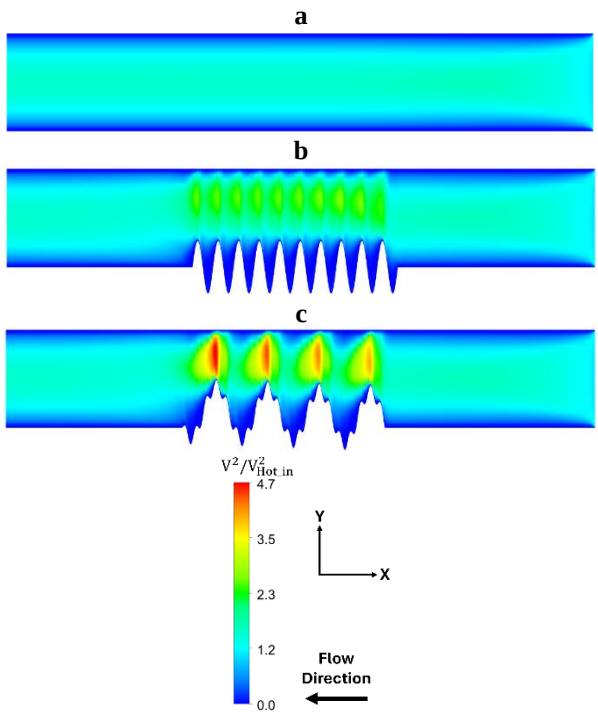

Figure 6. Normalized dynamic pressure at Re = 3500 for (a) Flat HX, (b) Single sine wave HX, and (c) Double sine wave HX

Figure 6 shows the contours of the normalized dynamic pressure inside the hot channels of the HX. The contours are normalized with the square of the inlet velocity to the hot channel. The dynamic pressure contours show the flow patterns inside the additively manufactured HX. The patterns of the sine wave HX show distinct flow regions inside the HX channel. As water flows over the sine wave corrugations, the dynamic pressure increases due to the reduced cross-sectional area, as shown in Figure 6(b). The dynamic pressure decreases when the water flows over the valleys of the sine wave corrugations since the cross-sectional area increases. This introduces a pattern of high and small dynamic pressures over the sine wave corrugations. Figure 6(c) shows a similar trend. However, the dynamic pressure is higher because of double sine wave corrugations.

Figure 7 shows the friction factor developed in the hot channel HX. Similar results happen in the cold channel HX. As expected, the channel with no corrugations has the lowest friction factor value. The values of the friction factor approximate the well-known relation for laminar flow in smooth channels as $64/\mathrm{Re}$. The single sine wave corrugations case increases the friction factor by almost twofold compared to the empty case. As expected, changing the case to a double sine corrugation (double 1 case) increases the friction factor. However, the increase in friction factor is only about 16%, but this increase is undesirable and will affect the thermal-

hydraulic performance negatively. When the frequency of the sine waves is reduced to halve the frequency of the double 1 case, the friction factor is reduced drastically in the double 2 case and becomes comparable with the empty case. This is an exciting result, as corrugations can be used without excess pressure drop.

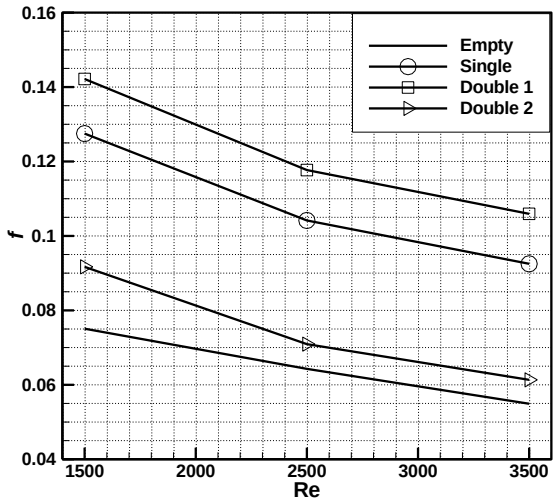

Figure 7. The friction factor in the hot channel HX versus Reynold number for the empty HX and the HXs with corrugations

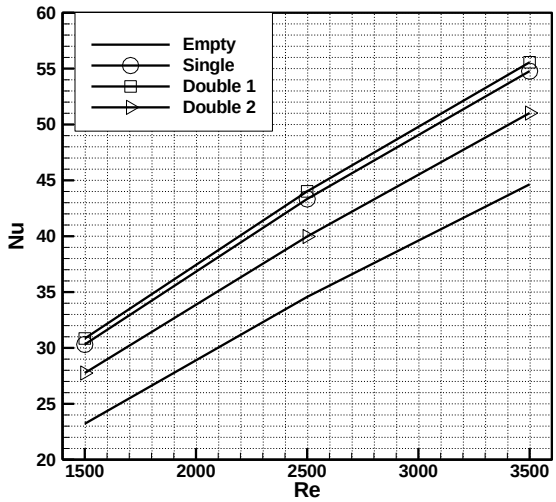

Figure 8. The Nusselt number in the hot channel HX versus Reynold number for the empty HX and the HXs with corrugations

Figure 8 shows the values of the Nusselt number as it varies with the Reynold number. The Nusselt number measures heat transfer enhancement by convection compared to pure conduction within a fluid. The empty case enhances the heat transfer more than pure conduction by more than 20 times. However, adding corrugations will allow us to improve the heat transfer even more. The single sine wave corrugations have doubled the heat transfer compared to the empty case. Among all the cases, the double 1 case performs the best. However, its improvement over the single sine wave corrugations is very slight. The double 2 case have a noticeable improvement in the Nusselt number compared to the empty case. However, it is considered the lowest compared to the other corrugated cases. As the flow rate increases, the Nusselt number increases for all the cases.

Figure 9 shows the thermal-hydraulic performance with the flow rate for the different corrugation cases. Thermal-hydraulic performance measures how well the heat exchanger performs in the presence of corrugations. It compares the enhancement of the Nusselt number and the increase in pressure drop to the empty case. The double 1 case has the lowest performance. Thermal-hydraulic performance decreases with the increase in flow rate. The double 2 case performs better than the other two cases. This performance is attributed to the small friction factor that developed in this case. The single-sine wave corrugations lie between the two double-sine wave corrugations. Having double since wave corrugations helps increase the thermal-hydraulic performance if the frequencies of the sine waves are not high.

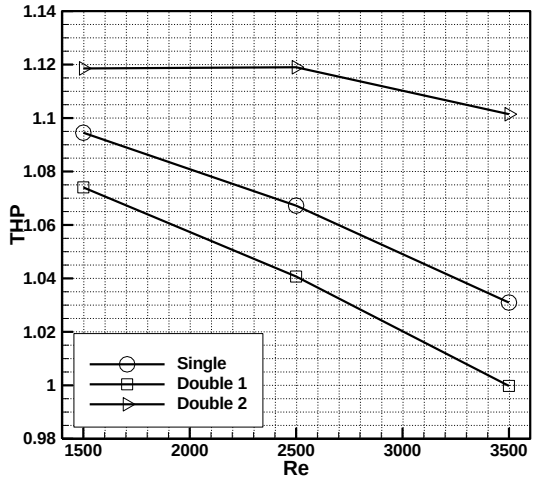

Figure 9. The thermal-hydraulic performance for the HX versus Reynold number with corrugations

The simulation results for different HX configurations are summarized in Table 3. For the empty channel, the Nusselt number (*Nu*) increased from 23.21 to 44.64 as the Reynolds number (*Re*) increased from 1500 to 3500, while the friction factor (*f*) decreased from 0.07507 to 0.05490. In the single sine wave corrugation case, the Nu values ranged from 30.31 to 54.77, indicating enhanced heat transfer due to induced turbulence. The friction factor for this configuration decreased from 0.12749 to 0.09251 as *Re* increased from 1500 to 3500, indicating relatively higher resistance to flow despite the increased heat transfer efficiency. The thermal-hydraulic performance (THP) for the single sine wave case showed values of 1.09, 1.07, and 1.03 for *Re*=1500, 2500, and 3500, respectively.

The double sine wave corrugations were tested in two configurations, Double 1 and Double 2. For Double 1, the Nu values ranged from 30.84 to 55.56, with friction factors decreasing from 0.14216 to 0.10593 as *Re* increased from 1500 to 3500. The THP values for Double 1 were 1.07, 1.04, and 1.00, showing a decline with increasing *Re*. For Double 2, the *Nu* values ranged from 27.75 to 51.02, with corresponding friction factors decreasing from 0.09169 to 0.06133. The THP for Double 2 remained relatively consistent at 1.12 for *Re*=1500 and 2500, and 1.10 for *Re*=3500, indicating better overall performance in heat transfer enhancement and thermal efficiency than the other configurations.

These results highlight the significant impact of sine wave corrugations on heat transfer performance, with Double 2 showing the most balanced improvement in heat transfer and pressure drop characteristics.

Table 3. Summary of Nusselt number, friction factor, and thermal hydraulic performance for various HX configurations at different Reynolds numbers

Case	*Re*	*Nu*	*f*	THP
Empty	1500	23.21	0.07507	-
	2500	34.57	0.06428	-
	3500	44.64	0.05490	-
Single	1500	30.31	0.12749	1.09
	2500	43.33	0.10415	1.07
	3500	54.77	0.09251	1.03
Double 1	1500	30.84	0.14216	1.07
	2500	44.01	0.11769	1.04
	3500	55.56	0.10593	1.00
Double 2	1500	27.75	0.09169	1.12
	2500	39.97	0.07092	1.12
	3500	51.02	0.06133	1.10

4. CONCLUSION

This article discusses the use of turbulators to enhance the heat transfer inside HX while maintaining a relatively low increase in pressure drop. The HXs will be made from polymer materials. Since traditional manufacturing techniques are limited in practicality, AM is the focus of manufacturing such HXs. Naturally, polymer materials have low thermal conductivity and poor heat conductors. However, they have other benefits, such as no corrosion, less fouling, and being lightweight. Nevertheless, using polymer-based HXs can be effective if new polymer materials have high thermal conductivity and the thickness of the HXs is small enough to reduce the thermal resistance to conduction. AM is an emerging technology used to overcome the difficulties found in traditional manufacturing technologies.

This paper introduces and simulates a novel HX surface configuration using CFD. The surface configuration comprises a complicated topology that can be described using a summation of sine wave terms. Due to the complexity of the several sine waves, only two sine waves are used to describe the topology of the HX surface. Each sine wave has an amplitude and a frequency, giving rise to several possibilities for the shape of the HX surface. Two surfaces with two sine waves are analyzed and simulated. The two surfaces are compared with a single sine wave corrugated HX surface and a plain HX surface.

The HX surface is simulated in Ansys Fluent to estimate the enhancement gained in heat transfer by adding the novel HX surface. The CFD model has been validated against experiments, and an extensive mesh study was applied. The results of this validation and mesh study were demonstrated in my previous publication. Due to the difficulties in CFD computations, the HX model was made using a 2D geometry. Since HX runs for long periods, steady-state simulations are used. Only two channels of a flat plate HX are used to demonstrate the applicability of the novel HX surface.

The main result of this study is that double sine wave corrugations could be a viable option in flat plate HXs. The amplitude of the sine wave corrugation should have a small height and a low frequency. This tends to increase the mixing inside the HX without giving rise to excessive pressure drop. The contour plots showed a good level of mixing near the HX surface in the streamwise direction. Secondary flow mixing might be present. However, 3D simulations are needed to show their presence.

The findings suggest that double sine wave corrugations in flat plate HXs can significantly enhance heat transfer efficiency while maintaining reasonable pressure drops. This can improve performance and cost savings in industrial applications where effective thermal management is critical. Specifically, industries such as HVAC, automotive, and energy sectors can benefit from the enhanced thermal management provided by these novel HX designs.

AM is gaining popularity, and several future works are needed to accelerate the progress in this technology. One of the difficulties is the structural integrity of 3D-printed parts. 3D printed parts are fragile and easy to break or degrade depending on the type of printing technology used and other printing factors and materials. Full-scale laboratory experiments are needed to test several HX conditions. Also, extreme conditions might affect 3D-printed HXs and are worthy of further investigation. Future studies should also optimize the design parameters to enhance heat transfer rates further and reduce material costs. Moreover, exploring the use of advanced polymer materials with higher thermal conductivity and developing multi-material printing techniques could open new trends for improving the performance and durability of 3D-printed HXs.

REFERENCES

[1] Cengel, Y.A. (2022). Heat Transfer a Practical Approach, Second Edi. Mcgraw-Hill.

[2] Nakhchi, M.E., Hatami, M., Rahmati, M. (2021). Experimental investigation of performance improvement of double-pipe heat exchangers with novel perforated elliptic turbulators. International Journal of Thermal Sciences, 168: 107057. https://doi.org/10.1016/J.IJTHERMALSCI.2021.107057

[3] Moria, H. (2023). A comprehensive geometric investigation of non-circular cross section spring-wire turbulator through the spiral-tube based heat exchangers. Results in Engineering, 17: 100906. https://doi.org/10.1016/J.RINENG.2023.100906

[4] Samruaisin, P., Maza, R., Thianpong, C., Chuwattanakul, V., Maruyama, N., Hirota, M., Eiamsa-ard, S. (2023). Enhanced heat transfer of a heat exchanger tube installed with V-shaped delta-wing baffle turbulators. Energies, 16(13): 5237. https://doi.org/10.3390/en16135237

[5] Wang, Z.Y., Wang, R.H., Li, Z., Wang, M., Wan, L. (2023). Numerical investigation on the effect of cylindrical turbulator on performance of corrugated plate-fin heat exchanger. Applied Thermal Engineering, 230(Part A): 120726. https://doi.org/10.1016/j.applthermaleng.2023.120726

[6] Saini, R., Gupta, B., Prasad Shukla, A., Singh, B., Baredar, P., Bisen, A. (2023). CFD analysis of heat transfer enhancement in a concentric tube counter flow heat exchanger using nanofluids (SiO_2/H_2O, Al2O3/H_2O, CNTs/H_2O) and twisted tape turbulators. Materialstoday: Proceedings, 76(Part 2): 418-429. https://doi.org/10.1016/j.matpr.2022.12.044

[7] Farajollahi, A., Mokhtari, A., Rostami, M., Imani, K., Salimi, M. (2022). Numerical study of using perforated conical turbulators and added nanoparticles to enhance heat transfer performance in heat exchangers. Scientia Iranica, 30(3): 1027-1038.

https://doi.org/10.24200/sci.2022.59717.6394
[8] Hegab, H., Khanna, N., Monib, N., Salem, A. (2023). Design for sustainable additive manufacturing: A review. Sustainable Materials and Technologies, 35: e00576. https://doi.org/10.1016/J.SUSMAT.2023.E00576
[9] Jasiuk, I., Abueidda, D.W., Kozuch, C., Pang, S., Su, F.Y., McKittrick, J. (2018). An overview on additive manufacturing of polymers. JOM, 70: 275-283. https://doi.org/10.1007/s11837-017-2730-y
[10] Campbell, I., Bourell, D., Gibson, I. (2012). Additive manufacturing: Rapid prototyping comes of age. Rapid Prototyping Journal, 18(4): 255-258. https://doi.org/10.1108/13552541211231563
[11] Pratama, A., Irwansyah, R. (2023). Additive manufacturing-based heat exchanger: A review. AIP Conference Proceedings, 2630: 030008. https://doi.org/10.1063/5.0125848
[12] Alshwairekh, A.M. (2023). A computational fluid dynamics study on polymer heat exchangers for low-temperature applications: Assessing additive manufacturing and thermal-hydraulic performance. International Journal of Heat and Technology, 41(3): 602-610. https://doi.org/10.18280/ijht.410312
[13] Lorenzon, A., Vaglio, E., Casarsa, L., Sortino, M., Totis, G., Saragò, G., Lendormy, E., Raukola, J. (2022). Heat transfer and pressure loss performances for additively manufactured pin fin arrays in annular channels. Applied Thermal Engineering, 202: 117851. https://doi.org/https://doi.org/10.1016/j.applthermaleng.2021.117851
[14] Menter, F.R. (1994). Two-equation eddy-viscosity turbulence models for engineering applications. AIAA Journal, 32(8): 1598-1605. https://doi.org/10.2514/3.12149
[15] Laitinen, A., Saari, K., Kukko, K., Peltonen, P., Laurila, E., Partanen, J., Vuorinen, V. (2020). A computational fluid dynamics study by conjugate heat transfer in OpenFOAM: A liquid cooling concept for high power electronics. International Journal of Heat and Fluid Flow, 85: 108654. https://doi.org/10.1016/j.ijheatfluidflow.2020.108654
[16] Li, K., Smith, T., Asher, W., Flores-Betancourt, A., Trofimov, A.A., Wang, H., Zhang, M., Kearney, L., Lara-Curzio, E., Ozcan, S., Kunc, V., Naskar, A.K., Nawaz, K. (2023). Additively manufactured polymer composites for heat exchanger applications: Evaluation of critical thermophysical properties. Journal of Materials Science, 58: 11585-11596. https://doi.org/10.1007/s10853-023-08709-8
[17] Ahmad, A., Abbas, A., Hussain, G., Al-Abbasi, O., Alkahtani, M., Altaf, K. (2023). Performance evaluation of 3D printed polymer heat exchangers: Influence of printing temperature, printing speed and wall thickness with consideration of surface roughness. The International Journal of Advanced Manufacturing Technology, 128: 3627-3647. https://doi.org/10.1007/s00170-023-12079-5
[18] Sankalp Shekar, S., Nagaraj, M., Mallashetty Shivamallaiah, M. (2023). Heat transfer augmentation of solar air heater using discrete transverse sinewave corrugations. Proceedings of the Institution of Mechanical Engineers, Part C: Journal of Mechanical Engineering Science, 238(5): 1778-1799. https://doi.org/10.1177/09544062231196089
[19] Liu, P., Sun, R., Hu, L., Wang, W., Ji, J. (2024). Heat Transfer enhancement of microchannel heat sink using sine curve fins. Journal of Thermophysics and Heat Transfer, 38(3): 1-12. https://doi.org/10.2514/1.T6967
[20] Du, J., Ren, F., Cai, Y., Shi, D., Zheng, S., Chu, X., Yu, X. (2022). Thermal performance analysis of triple casing latent heat system based on sinusoidal function type corrugation. Case Studies in Thermal Engineering, 36: 102168. https://doi.org/https://doi.org/10.1016/j.csite.2022.102168
[21] TCPOLY, Ice9 Flex TPU filament. https://Tcpoly.Com/Purchase-Ice9-Materials/.
[22] Alshwairekh, A.M., Alghafis, A.A., Alwatban, A.M., Alqsair, U.F., Oztekin, A. (2019). The effects of membrane and channel corrugations in forward osmosis membrane modules—Numerical analyses. Desalination, 460: 41-55. https://doi.org/10.1016/j.desal.2019.03.003

NOMENCLATURE

A	Area of the heat transfer surface in the heat exchanger, m^2
c	Specific heat, $\mathrm{J/kg \cdot K}$
D	Hydraulic diameter of the heat exchanger, m
h	Convective heat transfer coefficient, $\mathrm{W/m^2 \cdot K}$
k	Thermal conductivity, $\mathrm{W/m \cdot K}$
k_p	Polymer thermal conductivity, $\mathrm{W/m \cdot K}$
L	Length of HX surface, m
$\dot{m}$	Water mass flow rate, $\mathrm{kg/s}$
ΔP	Pressure difference along one channel of HX, Pa
$\dot{Q}$	Rate of heat transfer, W
R	Thermal resistance, $\mathrm{K/W}$
T	Temperature, K
t	HX surface thickness, m
U	Overall heat transfer coefficient, $\mathrm{W/m^2 \cdot K}$
V	Fluid velocity inside HX, $\mathrm{m/s}$
ρ	Fluid density, $\mathrm{kg/m^3}$
μ	Fluid viscosity, $\mathrm{N \cdot s/m^2}$